

AFOSR-TR. 79-0434

LEVEL

5

MODEL FOR STEADY-STATE COMBUSTION
OF UNIMODAL COMPOSITE SOLID PROPELLANTS

Merrill K. King

January, 1978

*See back page
p. 1473*

DDC
RECEIVED
APR 17 1979
C

DDC FILE COPY ADA067585

→ ATLANTIC RESEARCH CORPORATION
Research and Technology Division
5390 Cherokee Avenue
Alexandria, Virginia 22314

SIC 403338

Contract

F49620-78-C-0016

JM

Air Force Office of Scientific Research
Building 410
Bolling AFB, D.C. 20332

APPROVED FOR PUBLIC RELEASE; DISTRIBUTION UNLIMITED

79 04 13 074

AIR FORCE OFFICE OF SCIENTIFIC RESEARCH (AFSC)
NOTICE OF TRANSMITTAL TO DDC
This technical report has been reviewed and is
approved for public release IAW AFR 190-12 (7b).
Distribution is unlimited.
A. D. BLOSE
Technical Information Officer

MODEL FOR STEADY-STATE COMBUSTION OF UNIMODAL
COMPOSITE SOLID PROPELLANTS*

Dr. Merrill K. King**
Atlantic Research Corporation
Alexandria, Virginia 22314

Abstract

A model for prediction of burning rate-pressure-crossflow velocity relationships for non-metallized composite propellants containing unimodal oxidizer, given only composition and oxidizer particle size, has been developed. This model embodies many of the concepts used in the Beckstead-Derr-Price model, but contains major modifications, including a postulated columnar diffusion flame bending mechanism for erosive burning. The major part of this paper is devoted to description and discussion of these modifications and to model development. Preliminary predictions of burning rate at various pressures and crossflow velocities have been made for a series of three 73/27 ammonium perchlorate (AP)/hydroxy-terminated-polybutadiene (HTPB) formulations, with oxidizer particle diameters of 5, 20, and 200 microns, and compared with data for these formulations. With optimization of three free constants[†] appearing in the model, it is found to give excellent agreement with no-crossflow burning rate data over the entire range of pressures and particle sizes studied. In all cases, however, the predicted sensitivity of burning rate to crossflow velocity is somewhat less than observed experimentally.

Introduction and Background

As part of a program in which the sensitivity of composite propellant burning rate to crossflows is being experimentally and analytically studied, this author has developed a "first generation" model¹ for the prediction of burning rate-pressure-crossflow relationships for composite propellants which requires as input burning rate versus pressure data in the absence of crossflow. A more fundamental model (with explicit calculation of the distances of various heat release zones from the propellant surface rather than inference of these distances from zero crossflow data) of the propellant combustion process which permits prediction of burning rate versus pressure at various crossflow velocities (including zero crossflow), given only propellant composition and ingredient size data, is highly desirable. During the past year, this author has been working on development of such a model for the case of propellants containing unimodal ammonium perchlorate oxidizer and no metal additives (with plans to extend this model later to treat multimodal oxidizer and metallized propellant cases). Initially, it was planned to simply modify the Beckstead-Derr-Price (BDP) model^{2,3} (the most commonly accepted composite propellant combustion model, in various forms, in this country today) for pre-

*Research sponsored by the Air Force Office of Scientific Research (AFSC), United States Air Force, under Contracts F44620-76-C-0023 and F49620-78-C-0016. The United States Government is authorized to reproduce and distribute reprints for governmental purposes notwithstanding any copyright notation hereon.

**Chief Scientist, Research and Technology, Member AIAA.

diction of burning rates of composite propellants as a function of pressure (in the absence of crossflow) to allow for bending of the diffusion flame(s) considered in that model. However, upon careful review of the BDP model, this author found sufficient problems and areas of disagreement with that model that it was decided to develop an entirely new composite propellant combustion computer code (embodying many of the BDP concepts, while modifying or replacing others) with the flame-bending mechanism described in Reference 1 embedded in the mathematical analysis. Major modifications to the BDP model included are:

- 1) Variation in local oxidizer/binder surface area ratio as the propellant regresses past an oxidizer particle is considered. (In the BDP, an average ratio is used - this assumes that several very nonlinear processes can be linearly averaged.)
- 2) The kinetics of subsurface/surface exothermic reactions are considered, with use of rate expressions based upon the work of Waesche and Wenograd⁴. (In the BDP model, subsurface/surface heat release is included with the endothermic ingredient vaporization heats, with the resultant implicit assumption that the amount of heat release in these reactions per unit mass of propellant is independent of such parameters as burning rate.)
- 3) A correction of an inconsistency in definition of areas in the BDP model is made.
- 4) The calculation of the dimensionless stoichiometric group needed for calculation of the flame height via the Burke-Schumann⁵ analysis is modified. (The group used in the BDP model is inconsistent with that defined in the original work of Burke-Schumann.)
- 5) A two-flame (fuel-gas/oxidizer-gas columnar diffusion flame and ammonium perchlorate monopropellant flame), rather than a three-flame model, is used. (With correction of the calculation of the stoichiometry dimensionless group for the Burke-Schumann analysis, it no longer appears necessary to differentiate between the parts of the diffusion flame inside and outside of an ammonium perchlorate monopropellant flame.)
- 6) The procedure for calculation of heat feedback from the diffusion flame and the AP monopropellant flame is modified. (In the BDP model, all flames are considered to occur in flame sheets at discrete distances from the surface: in the current model, the AP monopropellant heat release is treated as a flame-sheet type heat release, but the diffusion flame heat release is considered to occur over a finite range of distances from the propellant surface.)
- 7) The distance (measured normal to the propellant surface) associated with oxidizer-binder gas interdiffusion in the presence of cross-

flow is assumed to be reduced by a factor, $\sin \theta$, where θ is the angle of the resultant of the crossflow and transpiration velocities (at the outer edge of the diffusion flame region) relative to the surface, as in the first generation model described in Ref. 1.

Model Development

A major assumption made in the BDP model (and variants thereof) is that one may work in terms of an average oxidizer-fuel ratio for a given size oxidizer particle. In reality, however, an oxidizer particle and the fuel surrounding it (and associated with it) will be receiving heat feedback from a diffusion flame of strongly varying oxidizer/fuel ratio during its burning. As the oxidizer particle first becomes exposed to the surface, with only its tip showing, the local oxidizer-fuel ratio will be quite low. As the burning surface passes the equator of the particle, however, the oxidizer-fuel ratio will be comparatively high, and as the particle burns out, the ratio will again be low. Implicit in the BDP use of an "average" oxidizer-surface planar intersectional area is the assumption that all of the highly non-linear dependencies of burning rate, flame temperature, and consequently heat feedback from the diffusion flame can be linearly averaged over the range of the variations during regression of the propellant surface through the oxidizer. Things may work out this way, but this appears to this author to be a somewhat risky a priori assumption. Accordingly, in this model (limited thus far to unimodal oxidizer) an attempt is made to allow for the variation in local oxidizer/fuel ratio associated with the burning of an individual oxidizer particle due to the variation in relative oxidizer-fuel surface intersectional areas as the surface regresses through the particle.

In deciding how to treat this variation (or, indeed, whether to treat it) one must first address the question of propellant surface and subsurface response to variation in heat feedback flux from the varying oxidizer/fuel gas-phase diffusion flame. If the burning rate response is very slow, such variations in feedback flux are damped out and the averaging procedure of BDP is probably adequate. If, on the other hand, response of burning rate variations to heat feedback flux variations is sufficiently fast, one may use quasi-steady state calculations of the burning rate at each fuel/oxidizer area ratio during the regression of the burning surface through the particle and then properly average these to arrive at an average burning rate. In between these extremes lies great difficulty. A transient heat conduction program allowing for surface ablation was employed to examine the response of ablation rate to variation in heat flux to the surface. Variations in heat flux up to 10^6 cal/cm² sec² (corresponding to approximate doubling of heat feedback flux from a typical steady-state value in 0.50 msec, the time required for a propellant burning at 2 cm/sec to regress 10 microns) were examined. In all cases, the burning rate response was found to track the feedback flux variation within 10 percent. Accordingly, it was concluded that use of a quasi-steady-state approach to calculation of propellant burning rate at various oxidizer/fuel ratios associated with different intersections of the propellant burning surface with a given oxidizer particle would not be seriously in error.

As mentioned earlier, this model is presently limited to unimodal oxidizer particle size. Having

concluded that one can use a quasi-steady-state approach to calculating burning rate as a function of the ratio of planar areas of oxidizer and associated fuel intersected by the regressing surface, one is next faced with the question of how to calculate the distribution of these areas. Since composite propellants are normally quite highly loaded with solid oxidizer in the rubber fuel binder, and since with unimodal oxidizer propellants the desire for these high loadings tends to lead to loadings approaching maximum theoretical loading, it was decided that as a reasonable approximation, one might assume a regular packing of oxidizer crystals in the binder corresponding to the arrangement of a cubic closest packing array, though with the spacing larger than that for a true cubic closest packing, corresponding to less than 100 percent of theoretical maximum loading. Simple geometrical considerations then permit one to calculate the characteristic lattice dimension D_1 (where lattice spacings in three mutually orthogonal planes are given by D_1 , $0.866 D_1$, and $0.82 D_1$) as:

$$D_1 = \left(\frac{0.737}{VLO} \right)^{1/3} D_o = \left(\frac{0.737 [WFO/\rho_{ox} + (1-WFO)/\rho_F] \rho_{ox}}{WFO} \right)^{1/3} D_o \quad (1)$$

It is arbitrarily assumed that the propellant burns in the direction in which the planes of oxidizer are separated by $0.82 D_1$. This distance is broken up into equally spaced increments and straightforward geometrical relations are then used to calculate the planar intersection area of the burning surface with the oxidizer (APOX) and its associated fuel planar area (AFU) at each of the intersection planes, with the assumption that wherever two layers of oxidizer overlap the fuel is apportioned between them in the ratio of their planar surface intersection areas. The result of these calculations is a table of planar oxidizer-surface intersectional area (APOX) and associated fuel surface area (AFU) versus distance of the intersection plane from the initial top of the particle (XDTOP). Results of a typical calculation are presented in Table 1. Burning rates for each of these conditions (starting at the top of the particle since one must allow for different regression rates of fuel and oxidizer) are then calculated as described below and an averaging procedure, also described below, is then used to calculate an average propellant burning rate.

Next let us address the question of calculation of propellant burning rate at each of the conditions defined by the various distances of the burning surface intersection plane from the top of the oxidizer particle, as listed for the example in Table 1. First, since as mentioned above, different oxidizer and fuel regression rates are to be allowed, one must address rather carefully the questions of surface geometry and mass conservation at the surface. In this model, as in the BDP model, the fuel is assumed to regress in a planar manner, and the oxidizer-fuel surface is forced to be continuous at their intersection. These restrictions, coupled with the fact that the linear regression rates of fuel and oxidizer perpendicular to their directions of regression are allowed to differ, force the oxidizer surface to assume a curved shape as it regresses. Oxidizer mass fluxes may be expressed relative to either the actual curved surface area or the planar projection of this area, the two values being related by:

$$\dot{m}_{ox,p} (APOX) = \dot{m}_{ox,s} (ASOX) = \frac{r}{\rho_{ox}} (ASOX) \quad (2,2a)$$

The area-average mass flux of fuel and oxidizer normal to the mean regression plane is given by:

$$\dot{m} = \frac{\dot{m}_{\text{fuel}}(\text{AFU}) + \dot{m}_{\text{ox,p}}(\text{APOX})}{\text{AFU} + \text{APOX}} \quad (3)$$

$$= \frac{\dot{m}_{\text{fuel}}(\text{AFU}) + \dot{m}_{\text{ox,s}}(\text{ASOX})}{\text{AFU} + \text{APOX}}$$

It is important to know the value of ASOX at each plane since the Arrhenius expression relating oxidizer mass flux to surface temperature must be written in terms of $\dot{m}_{\text{ox,s}}$ to be meaningful:

$$\dot{m}_{\text{ox,s}} = B_{\text{ox}} \exp(-E_{\text{ox}}/RT_s) \quad (4)$$

A similar expression for the fuel pyrolysis rate:

$$\dot{m}_{\text{fuel}} = B_{\text{fuel}} \exp(-E_{\text{fuel}}/RT_s) \quad (5)$$

enables one to calculate the ratio of oxidizer and fuel regression rates as a function of surface temperature:

$$\frac{r_{\text{ox}}}{r_{\text{fuel}}} = \frac{\dot{m}_{\text{ox,s}} \rho_{\text{fuel}}}{\dot{m}_{\text{fuel}} \rho_{\text{ox}}} \quad (6)$$

$$= \frac{\rho_{\text{fuel}} B_{\text{ox}} \exp(-E_{\text{ox}}/RT_s)}{\rho_{\text{ox}} B_{\text{fuel}} \exp(-E_{\text{fuel}}/RT_s)}$$

There is considerable uncertainty as to best values to be used for B_{ox} , B_{fuel} , E_{ox} , and E_{fuel} : thus, parametric study of the effects of these values is required. Note that it has been assumed here that the oxidizer and fuel surface temperatures are equal. This is probably not a particularly good assumption, but relaxing it requires a rather complex three-dimensional heat transfer analysis.

Now, how does one go about calculating ASOX for succeeding regression intervals through the oxidizer particle? First, it is assumed (approximated) that at the first increment after the tip of the particle becomes exposed (in Table 1, when the distance from the top of the particle is 0.119 microns) the oxidizer surface is planar. The procedure outlined below for calculation of burning rate, given the local oxidizer/fuel area ratio, is then used to calculate the oxidizer and fuel linear regression rates under the conditions given for this first increment. The fuel regression rate is then used to calculate the time for the regressing fuel to reach the second increment (distance from the initial particle top of 1.017 microns in Table 1) as:

$$\text{TAU}_2 = (\text{XDTOP}_2 - \text{XDTOP}_1) / r_{\text{fuel}} \quad (7)$$

The distance which the center of the AP particle peak regresses in that time is then calculated as:

$$\Delta(\text{DELOX}) = r_{\text{ox}}(\text{TAU}_2) \quad (8)$$

Similar procedures are followed for each succeeding increment, yielding for each XDTOP (distance of fuel surface from the initial top of the oxidizer particle) a value of DELOX (distance of the center of the oxidizer surface from the initial top). The geometrical method depicted in Figure 1 (and discussed in detail in References 3 and 6) then permits calculation of the actual curved oxidizer surface area, ASOX, as:

$$\text{ASOX} = \pi[(\text{XDTOP})D_o - 2(\text{XDTOP})(\text{DELOX}) + \text{DELOX}^2] \quad (9)$$

For the calculation of the length of the columnar diffusion flame between fuel gases from the

binder pyrolysis and oxidizer gases from the oxidizer decomposition (discussed later) several other parameters associated with the surface configuration of the oxidizer particle-associated fuel combination at each increment must be calculated. First, the combined radius of the oxidizer and binder gas streams (in this model, a modified Burke-Schumann analysis with a fuel annulus surrounding an oxidizer gas core is employed for the columnar diffusion flame calculation) is calculated as:

$$R_{\text{BS}} = \sqrt{(\text{AFU} + \text{APOX})/\pi} \quad (10)$$

In line with the requirement in the Burke-Schumann analysis that the linear velocity of the fuel and oxidizer streams have the same initial value, the oxidizer and fuel gas streams leaving the surface are assumed to adjust their areas quickly from the planar areas of the solids to meet this requirement. Since the temperature at the surface is assumed to be the same for the fuel and oxidizer, and pressures are equal, this leads to an expression for the radius of the inner oxidizer gas jet of:

$$L_{\text{BS}} = R_{\text{BS}} \left/ \left(1 + \frac{\dot{m}_{\text{fuel}}(\text{AFU})(\text{MW})_{\text{ox}}}{\dot{m}_{\text{ox,s}}(\text{ASOX})(\text{MW})_{\text{fuel}}} \right)^{1/2} \right. \quad (11)$$

The linear gas velocity away from the surface, also required in the modified Burke-Schumann analysis, as well as for calculation of characteristic reaction distances (products of reaction times and this velocity) is calculated as:

$$V_{\text{gas,surf}} = \frac{\dot{m}_{\text{ox,s}}(\text{ASOX})RT_{\text{surf}}}{(\text{MW})_{\text{ox}} \pi (L_{\text{BS}})^2} \quad (12)$$

Finally, the ratio of the molar fuel/oxidizer ratio to stoichiometric molar fuel/oxidizer ratio for the combined fuel and oxidizer streams (ϕ), also required in the modified Burke-Schumann analysis, is calculated as:

$$\phi = \frac{C_2}{1C_1} \frac{R_{\text{BS}}^2 - L_{\text{BS}}^2}{L_{\text{BS}}^2} \quad (13)$$

Since the initial pressure and temperature of the fuel and gas streams are the same, the concentration ratio C_2/C_1 may be replaced by a ratio of mole fractions Y_2/Y_1 . With subsurface reactions, the fuel mole fraction is reduced by a factor $(1-\beta)$ from its value in the absence of any subsurface reactions, while the oxidizer mole fraction is reduced from its no-subsurface-reaction value by a factor $(1-\alpha)$. With these substitutions, Equation 13 becomes:

$$\phi = \frac{Y_{2,o}(1-\beta)(R_{\text{BS}}^2 - L_{\text{BS}}^2)}{1 Y_{1,o}(1-\alpha) L_{\text{BS}}^2} \quad (14)$$

The burning rate of the propellant at any given set of oxidizer/fuel conditions (any regression increment) is controlled by heat released (exothermic reactions) at various locations. In this model, we consider three principal heat release zones: (1) heat release in a thin subsurface zone quite near (and including) the propellant surface; (2) heat release in the gas-phase above the propellant from ammonium perchlorate decomposition products burning as a monopropellant; and (3) heat release from a diffusion flame between AP decomposition (and monopropellant flame) products and fuel vapor released

by binder pyrolysis.

The subsurface/surface heat release is calculated by an iterative process, coupled with the remainder of the model, in which an estimate of the subsurface temperature profile is made and substituted into an Arrhenius rate expression representing subsurface heat release rate data measured by Waesche and Wenograd⁴, which is then integrated from the surface deep into the unburned propellant to obtain the total subsurface heat release per unit mass of propellant. This procedure differs markedly from that of the BDP model, in which the amount of subsurface heat release per unit mass of propellant is assumed to be a constant, independent of such parameters as burning rate, and is included with the binder heat of vaporization. Since the subsurface temperature profile steepens rapidly with increasing burning rate, while surface temperature increases with burning rate, our procedure results in the subsurface heat release per unit mass of propellant varying with burning rate. As will be discussed later, the surface energy balance in this model is written with the surface area of the oxidizer and associated fuel as the basis: thus all terms appear in the units of energy/time. For book-keeping convenience, the surface/subsurface heat release term is written as:

$$\dot{q}_{sub} = \dot{m}_{ox,s} (ASOX) Q_{EXO} \alpha \quad (15)$$

It is assumed that a stoichiometric amount of fuel is reacted with the oxidizer in these surface/subsurface reactions. Thus the fraction of fuel reacted in these reactions, β , is given by:

$$\beta = SMRBO \frac{\dot{m}_{ox,s} (ASOX)}{\dot{m}_{fuel} (AFU)} \alpha \quad (16)$$

Based upon Waesche and Wenograd subsurface reaction rate data, the fraction of oxidizer reacted per unit time is given for AP/CTPB systems as a function of temperature by:

$$R_{\alpha} = B_{Sub} \exp(-E_{sub}/RT) \quad (17)$$

with preliminary examination of their data indicating that the activation energy is approximately 40,000 calories/mole, while the pre-exponential is approximately $2.5 (10^{11})$. (As will be discussed later, however, use of these values leads to very little predicted subsurface heat release which in turn leads to underprediction of burning rate for formulations containing large oxidizer particles: accordingly, somewhat higher values of the pre-exponential factor were also examined.) The unperturbed (uncoupled) subsurface temperature profile is given by:

$$T = (T_s - T_0) \exp(r_{ox} \rho_{ox} C_{pox} x / \lambda_{ox}) + T_0 \quad (18)$$

Substitution of Equation 18 into Equation 17 and integration of:

$$\alpha = \int_{x=0}^{x'} \frac{R_{\alpha} dx}{r_{ox}} \quad (19)$$

where x' represents a distance below the surface at which the reaction rate has dropped to 1 percent of its surface value, yields, with use of several approximations:⁶

$$\alpha \approx \frac{B_{sub} \lambda_{ox} c_{pox}^{-1} \exp(-E_{sub}/RT_s) \left[1 - \exp(-0.25 E_{sub} (T_s - T_0) / RT_s^2) \right]}{r_{ox} \rho_{ox} C_{pox} E_{sub} (T_s - T_0)} \quad (20)$$

Thus Equation 20 relates the mass fraction of oxidizer reacting exothermically at or below the surface to the surface temperature and linear regression rate of the oxidizer.

As regards gas-phase heat release zones, a two-flame approach was chosen for this model, the two flames being an AP monopropellant flame and a columnar diffusion (Burke-Schumann) flame. The reasons that a two-flame rather than a three-flame model (as the BDP) was chosen were:

- 1) Mathematical simplification.
- 2) Lack of apparent difference in a diffusion flame between AP decomposition products and fuel and a flame between AP monopropellant flame products and fuel. In both cases, the overall stoichiometry is the same, while AP decomposition products bring more oxidizer into a binder fuel stream than do AP monopropellant flame products, they also bring more fuel, with the result that the overall mixture ratio at a given point is nearly the same.
- 3) Provisions were made in calculation of the AP monopropellant heat release to allow for consumption of reactants for that flame in part of the columnar diffusion flame which occurred inside the AP flame.

Three distance parameters are important in calculating heat feedback from these gas flames to the propellant surface. These are pictured in Figure 2. These distances are designated as $FH90 \sin \theta$, L_{AP} and L_{RX} . $FH90$ refers to the distance associated with completion of 90 percent of the mixing of fuel and oxidizer gas products. (If there were no reaction delay, this would be equivalent to the 90 percent heat release point.) L_{RX} refers to the reaction distance associated with the binder gas-oxidizer gas flame, and L_{AP} refers to the reaction distance associated with the monopropellant AP product flame (both being characteristic reaction times multiplied by the gas velocity away from the surface). As discussed in Reference 1, flame bending associated with crossflow is assumed to reduce the distance from the surface to the end of the columnar diffusion heat release (90 percent point) by reducing $FH90$ to $FH90 \sin \theta$, measured perpendicular to the surface, where θ is the angle between the surface and the resultant vector of the transpiration and crossflow velocities at the outer edge of diffusion flame zone. $FH90$ is calculated as a function of various parameters using a modified Burke-Schumann analysis as described below. A series of calculations of $FH90$ as a function of these parameters was performed externally and correlations of the results were used in the final program. In this model, it is assumed that the fraction of planar projection of surface, $A_{POX}/(A_{POX} + A_{FU})$ receives flux from both AP monopropellant and columnar diffusion flames (the latter at the adiabatic flame temperature, T_f , which is a function of the oxidizer/fuel ratio, $\dot{m}_{ox,s} [ASOX] / \dot{m}_{fuel} [AFU]$) while the remaining fraction of the surface receives flux only from this diffusion flame; however, these fluxes are assumed to smear out uniformly in the propellant. Thus, the total heat flow from the gas-phase heat release zones is given as:

$$\dot{q}_{\text{gas}} = \text{APOX } (\dot{q}_{\text{series flames}}) + \text{AFU } (\dot{q}_{\text{diffusion flame}}) \quad (21)$$

Heat release from the AP monopropellant flame is assumed to be a planar one, resulting in a discontinuity in the temperature derivative at its point of release, while the columnar diffusion flame is assumed to release its heat uniformly between $x = L_{RX}$ and $x = L_{RX} + FH90 \sin \theta$. (Actually, detailed examination of the Burke-Schumann flame structure indicates that this heat release should be more heavily weighted toward the inner side of this zone - this will be discussed further later in the paper.) With use of multitudinous algebraic manipulations, we arrive at the following expressions for the heat fluxes at the surface (allowing for reduction of reactants available for the AP monopropellant reaction by occurrence of some diffusion flame reaction closer to the surface):

$$\dot{q}_{\text{diffusion flame}} = \frac{\dot{m} C_p (T_f - T_s)}{z_1 - 1} \times \quad (22)$$

$$\left[1 - \frac{e^{z_1} \{1 - (e^{z_2} - 1)\}}{z_2} \right] \left[\frac{e^{z_1} - (e^{z_2} - 1)}{z_2} \right]$$

$$\dot{q}_{\text{series flames}} = \dot{q}_{\text{diffusion flame}} \quad (23)$$

$$+ \frac{\dot{m} Q_{AP} (1-\alpha) \left[1 - \frac{L_{AP} - L_{RX}}{FH90 \sin \theta} \right] \left[z_2 e^{z_3} - e^{z_2} + 1 \right]}{(z_2 e^{z_1} - e^{z_2} + 1)}$$

$$z_1 = \frac{\dot{m} C_p (L_{RX} + FH90 \sin \theta)}{\lambda}$$

$$z_2 = \frac{\dot{m} C_p FH90 \sin \theta}{\lambda}$$

$$z_3 = \frac{\dot{m} C_p (FH90 \sin \theta + L_{RX} - L_{AP})}{\lambda}$$

Next, let us consider the calculation of the distances L_{RX} , L_{AP} , and $FH90$ (and $FH90 \sin \theta$). The distance $FH90$, which is calculated from a modified Burke-Schumann columnar diffusion flame analysis (modified to allow for axial diffusion) is defined as the distance from the starting plane at which 90 percent of the fuel (for oxidizer-rich cases) or 90 percent of the oxidizer (for fuel-rich cases) will be consumed, assuming infinite reaction kinetics. This definition of the characteristic diffusion distance differs from that of the BDF model where the characteristic distance is defined as the distance from the starting plane to the point of closure of the flame over the oxidizer (fuel-rich cases) or the fuel (oxidizer-rich cases). One serious problem with use of the flame closure point to define the characteristic distance is that it has a singularity for stoichiometric situations: that is, for stoichiometric oxidizer-fuel ratio, the flame does not close and this characteristic distance goes to infinity. Since most of the heat is still released fairly close to the surface, this latter definition of a characteristic diffusion distance leads to seriously misleading results as regards heat feedback to the propellant surface at near stoichiometric oxidizer-fuel ratios: at oxidizer-fuel ratios far from stoichiometric, $FH90$ and the distances associated with flame closure

differ only slightly. Details of the calculation of $FH90$ are discussed in Reference 6. This parameter is a function of four independent parameters: the oxidizer jet radius, the equivalence ratio, the ratio of the outer radius of the fuel annulus to the oxidizer jet radius, and the ratio of diffusivity to transpiration velocity (evaluated at $T = (T_s + T_f)/2$).

$$FH90 = f_1 \left(\frac{L_{BS}}{D}, \frac{D}{V_{\text{gas}}}, \phi, \frac{R_{BS}}{L_{BS}} \right) \quad (24)$$

An extensive set of calculations covering a wide range of each of these variables was carried out externally to the final computer code and tabulations and correlations of the results were built into the final combustion model.

The reaction distances, L_{RX} and L_{AP} , are calculated as the products of reaction times and gas velocity away from the surface. Using the Zeldovich approach for premixed flame analysis along with several minor approximations which will not be detailed here, we arrive at for the oxidizer-fuel reaction distance, L_{RX} :

$$L_{RX} = \frac{K_{OF} V_{\text{gas, surf}} (1+\phi)^2 T_f^2 (\exp[E_{ACT, OF}/RT_f])}{p^{(n-1)} \phi} \quad (25)$$

For the ammonium perchlorate reaction distance, we find, neglecting variation of temperature at the AP heat release site (probably not a very bad approximation due to the low activation energy associated with the ammonia-perchloric acid reaction):

$$L_{AP} = \frac{K_{AP} V_{\text{gas, surf}}}{p^{n-1}} \quad (26)$$

The same approach to calculation of $\sin \theta$ as used in the previously mentioned first generation erosive burning model¹ was used in this model, the resulting equations being:

$$U_{\text{gas, x} = FH90 \sin \theta} = V_{\text{gas, surf}} \frac{T_f}{T_s} \quad (27)$$

$$Y^+ = \frac{10.5 (FH90 \sin \theta) (\bar{U}_{\text{crossflow}})^{0.9} T_f^{0.9} p^{0.9}}{D_{\text{channel}}^{0.1} ([T_s + T_f]/2)^{1.8}} \quad (28)$$

($FH90$ in microns; \bar{U} in ft/sec; D in ft; T in °K; p in atm)

$$\left. \begin{aligned} U^+ &= Y^+ \text{ for } Y^+ < 5 \\ U^+ &= -3.05 + 5.00 \ln Y^+ \text{ for } 5 \leq Y^+ \leq 30 \\ U^+ &= 5.5 + 2.5 \ln Y^+ \text{ for } Y^+ > 30 \end{aligned} \right\} \quad (29)$$

$$U_{\text{crossflow, x} = FH90 \sin \theta}^+ = \left[\frac{0.023 (\bar{U}_{\text{crossflow}})^{0.9} T_f^{0.18}}{D_{\text{channel}}^{0.1} p^{0.1}} \right] \quad (30)$$

$$\exp(-60 U_{\text{gas, x} = FH90 \sin \theta} / \bar{U}_{\text{crossflow}})$$

$$\sin \theta = \frac{U_{\text{gas, x} = FH90 \sin \theta}}{\sqrt{U_{\text{gas, x} = FH90 \sin \theta}^2 + U_{\text{crossflow, x} = FH90 \sin \theta}^2}} \quad (31)$$

As mentioned earlier, the final flame temperature, T_f , depends on the relative flow rates of fuel

and oxidizer gases at each calculational increment during progression of the propellant surface through the oxidizer. Accordingly, a table of flame temperature calculated with a thermochemical equilibrium program versus a parameter representing the relative flow rates is generated for the propellant system of interest (e.g., HTPB-AP) and included as a tabular look-up in the final program in the form:

$$T_f = f_2 \left(\frac{\dot{m}_{ox,s} ASOX}{\dot{m}_{fuel} AFU} \right) \quad (32)$$

In addition, the product gas heat capacity is somewhat dependent upon this parameter and an additional tabular look-up, based on thermochemical calculations, is included.

$$C_p = f_3 \left(\frac{\dot{m}_{ox,s} ASOX}{\dot{m}_{fuel} AFU} \right) \quad (33)$$

At this point, we have 26 equations (2,2a,3-6, 10-12, 14-16,20-33) in 27 unknowns ($\dot{m}_{ox,p}$, $\dot{m}_{ox,s}$, r_{ox} , \dot{m} , \dot{m}_{fuel} , T_s , r_{fuel} , RBS , $V_{gas,surf}$, ϕ , C_p , α , β , q_{sub} , q_{gas} , $q_{series\ flames}$, $q_{diffusion\ flame}$, LBS , LAP , LRX , θ , T_f , $U_{gas,x=FH90\ sin\ \theta}$, Y^* , U^* , $U_{crossflow,x=FH90\ sin\ \theta}$). For closure of the problem, we finally write an energy balance at the propellant surface as:

$$\begin{aligned} & \dot{m}_{fuel} (AFU) [C_{p,fuel} (T_s - T_o) + Q_{melt,fuel}] \\ & + \dot{m}_{fuel} (AFU) Q_{fuel\ vap} (1 - \beta) \\ & + \dot{m}_{ox,s} (ASOX) [C_{p,ox} (T_s - T_o) + Q_{melt,ox}] \\ & + \dot{m}_{ox,s} (ASOX) Q_{subl} (1 - \alpha) = \dot{q}_{sub} + \dot{q}_{gas} \end{aligned} \quad (34)$$

The resulting 27 equations (some of which, as mentioned, are tabular look-ups or correlations of one parameter as a function of others) are solved simultaneously in a computer program for each given set of values of ASOX and AFU associated with each surface regression increment. Among the outputs of each solution are values for r_{ox} , and r_{fuel} which are used in calculation of ASOX from the known APOX for the succeeding increment via Equations 7-9.

In the solution procedure, the thermal conductivity of the gas and the ratio of diffusivity to gas velocity (one of the independent parameters in Equation 24), both proportional to the square root of temperature, are evaluated at the average of the flame and surface temperature.

As the program is stepped through the succeeding increments of fuel plane distance from the initial top of the oxidizer particle (see Table 1), the oxidizer surface will either assume a protruding bulge or a depression relative to the planar fuel around it, depending upon whether the oxidizer linear regression rate is slower or faster than the binder regression rate. This raises interesting questions regarding the "end-game" if the particle burns out before the surrounding fuel. (Geometrical considerations show that the inverse problem cannot occur as long as increment sizes are kept sufficiently small.) In this case, there is no oxidizer to burn with the surrounding fuel in succeeding increments and the burning rate is set equal to zero for these remaining increments. Three different approaches have been taken to calculating the average propellant burning rate from the information obtained during the procedure of stepping through

the increments of regression of the fuel planar surface past the oxidizer particle (XDTOP increments). In the first of these, the burning rate is calculated by statistically averaging all of the oxidizer mass fluxes and fuel mass fluxes over the increments and dividing by the propellant density:

$$r_{avg} = \frac{\sum_j (\dot{m}_{ox,p,j} APOX_j + \dot{m}_{fuel,j} AFU_j)}{\rho_{propellant} \sum_j (APOX_j + AFU_j)} \quad (35)$$

while in the second approach it is calculated by statistically averaging all of the oxidizer mass fluxes and then dividing by the overall oxidizer mass fraction and the propellant density:

$$r_{avg} = \frac{\sum_j \dot{m}_{ox,p,j} APOX_j}{\rho_{propellant} WFO \sum_j (APOX_j + AFU_j)} \quad (36)$$

The fact that these two procedures do not always give the same result (though the differences are generally small) is tied in with the "end-game" problem mentioned above. If the oxidizer burns out before the fuel plane reaches the bottom of the oxidizer, mass fluxes for succeeding increments are set equal to zero in the procedure currently used. Not only does this result in different answers by the two above procedures, but it also pulls the average burn rates down. One's first temptation is to simply perform the summing procedure over just these increments for which a burning rate is calculated, both in the numerator and denominator of Equations 35 and 36, but it is not clear whether or not this is more physically realistic than the procedure of summing over all increments, with burning rate set equal to zero for increments in which there is no oxidizer for the fuel. A third procedure of calculating average burning rate was developed which basically does take this alternate approach, however, though in a slightly different manner. In this procedure, the burning rate is calculated by dividing the oxidizer particle diameter by the sum of the times required for each increment until the bottom of the oxidizer particle is reached:

$$r_{avg} = \frac{D_o}{\sum_j \tau_{TAU_j}} = \frac{D_o}{\sum_j [(\Delta(DELOX))_j / r_{ox,j}]} \quad (37)$$

This procedure begs the question of what happens to the fuel "left over" when the oxidizer particle burns out before the fuel. Physically we can perhaps just assume that it somehow flakes off. This question needs to be addressed further. This third approach does allow for the fact that the particle will spend more time at regression increments where the burning rate is lower, while the first two procedures involve an implicit assumption that each of the regression increments is equally likely.

Preliminary Results

During the past year, Atlantic Research has collected extensive experimental burning rate-pressure data in the presence of and absence of cross-flow for three non-metallized composite formulations containing unimodal ammonium perchlorate (AP) oxidizer. All three of these formulations consist of 73 weight percent AP and 27 weight percent hydroxyterminated-polybutadiene (HTPB) binder (with a trace of carbon black to opacify them). One of the formulations, designated as Formulation 4685, contains 5 micron diameter AP; the second, Formulation 4525, contains 20 micron diameter AP; and the third, Formulation 5051, contains 200 micron diameter

AP. Preliminary testing of the model described above has been carried out against burning rate data obtained for these three formulations. As may be seen from the above equations, numerous physical constants (e.g. heat capacities, densities, thermal conductivities, stoichiometry parameters, reaction heats, and rate constants) must be estimated for use of the model. Values for all but four of these parameters, estimated for the case of HTPB binder and AP oxidizer, appear in Table 2. Discussion of the estimation of these parameters appears in Reference 6. Of these parameters, the coefficient for the diffusivity expression is the least certain, since this value strongly depends on the nature of the reacting gas species and their products. It is estimated that this coefficient should lie somewhere between $1.0(10)^{-5}$ and $2.5(10)^{-5}$; the former value was chosen for the calculations presented in this paper. Four parameter values are not listed in Table 2: these are the gas reaction distance constants K_{AP} and K_{OF} , the pre-exponential term for the subsurface reaction B_{sub} , and the gas-phase reaction order n . During the course of this study gas-phase reaction orders of 1.8 and 2.0 were used: at this stage the former value appears to give better results and was used in all the predictions presented in this paper. Based on crude estimation procedures discussed in Reference 6, it was felt that K_{AP} should probably lie between approximately .00003 and .00015 $\text{atm}^{0.8} \text{ sec}$ for a reaction order of 1.8, or .00005 and .0003 atm sec for a reaction order of 2.0. A very crude estimate of K_{OF} indicates that it should lie between $0.3(10)^{-13}$ and $1.5(10)^{-13} \text{ atm}^{0.8} \text{ sec}/^\circ\text{K}^2$ for a reaction order of 1.8. Various values of these two parameters within these ranges were tried in attempts to fit the experimental burning rate data with one set of constants over the wide ranges of pressure, crossflow velocity, and particle size experimentally studied.

As mentioned earlier, our preliminary examination of Waesche and Wenograd⁴ subsurface reaction rate data indicated that the fraction of oxidizer reacted per unit time in AP/CTPB (and presumably AP/HTPB) systems could be expressed as $R_{\alpha} = 2.5(10)^{11} e^{-40000/RT}$. Accordingly, in our first attempts at using the model described above, we employed a value for B_{sub} of $2.5(10)^{11}$. With this value, we were able to find a set of values of K_{AP} and K_{OF} which gave good agreement between theory and experiment for zero crossflow for the 5 micron and 20 micron AP formulations, as shown in Figures 3 and 4. However, the model did tend to underpredict the effect of crossflow and, more important, resulted in gross underprediction of the burning rate and the burning rate-pressure slope for the no-crossflow case for the 200 micron AP formulation. (Figure 5) In all of these cases, the fraction of oxidizer and fuel consumed in subsurface reactions was predicted to be quite small (on the order of 1 to 2 percent).

Study of this problem of underprediction of burning rate of the 200 micron AP formulation indicated that it might be corrected by one or both of two possible modifications to the model, only one of which has been examined thus far. As mentioned earlier, the fuel gas - oxidizer gas diffusion flame is assumed to release its heat uniformly between $X = L_{RX}$ and $X = L_{RX} + FH90 \sin \theta$. (Figure 2). Detailed examination of reactant concentration profiles in the diffusion flame as predicted by the Burke-Schumann analysis indicate that in reality the heat release should be weighted fairly heavily toward the $X = L_{RX}$ side of this zone, tapering off

toward $X = L_{RX} + FH90 \sin \theta$. To allow for this in the model, alternate expressions to Equations 22 and 23 relating gas-phase heat feedback fluxes to $FH90 \sin \theta$, L_{RX} , and L_{AP} would have to be derived and substituted: this has not yet been done. It can be logically deduced that such a modification would reduce the predicted dependency of burning rate on oxidizer particle size, thus perhaps permitting good fitting of the 5, 20, and 200 micron AP formulation data with one set of constants.

The second approach which should also lead to decreased dependency of predicted burning rate on oxidizer particle size is to increase the predicted subsurface heat release by altering one or both of the constants in Equation 17. Since the Waesche and Wenograd⁴ data were obtained at relatively low temperatures (on the order of 600-700°K compared to typical predicted burning propellant surface temperatures of 900-1000°K) use of the expression fitted to their data does involve a dangerous degree of extrapolation. Moreover, while an activation energy of 40,000 calories/mole was employed in making this extrapolation, values ranging from 40,000 to 60,000 calories/mole appear in various reports by these authors. If one fixes the rate of reaction measured at 600°K and uses activation energies of 40,000, 50,000, and 60,000 calories/mole to extrapolate to 950°K, one predicts rates at that temperature in the ratio of 1 to 23 to 480. Accordingly, the value of B_{sub} was allowed to be a free parameter in further optimization of constants for the model. Though the best procedure would have been to simultaneously alter E_{sub} so as to give the same predicted rate at 600-650°K, in this preliminary examination E_{sub} was held constant at 40,000 calories/mole. With a value for B_{sub} of $5.2(10)^{12}$ (approximately 20 times the value initially used) the results shown in Figures 6 - 8 were obtained. As may be seen, the agreement between experiment and prediction is excellent for the no-crossflow cases across the entire range of pressure and particle size studied, though the effect of crossflow is still underpredicted. With this value of B_{sub} , on the order of 25 to 50 percent of the oxidizer is predicted to be consumed in subsurface/surface reactions.

It should be emphasized that these results are quite preliminary. Further examination of the subsurface reaction rate term and of the distribution of heat release in the fuel-oxidizer diffusion flame will be carried out. In addition, the question of choice of a proper averaging procedure for burn rate versus regression increment will be further examined.

Summary

A model for prediction of burning rate-pressure-crossflow velocity relationships for non-metallized composite propellants containing unimodal oxidizer, given only composition and particle size, has been developed. Data for three such propellants of identical composition (73/27 AP/HTPB) containing different sizes of unimodal oxidizer (5, 20, and 200 micron diameter) have been used for optimization of three free constants in the model. In a first effort, only two constants, those relating gas flame reaction distances to gas velocity away from the surface and pressure, were varied in a search for optimum values, the reaction constant for exothermic subsurface reactions being held at a value based on extrapolation of DSC data obtained by Waesche and Wenograd⁴. In this case a set of constants was found which yielded good agreement between experiment

and theory for the no-crossflow case for the 5 and 20 micron diameter AP formulations, but seriously underpredicted burning rates for the 200 micron AP formulation. Examination of the problem indicated that either use of a higher rate constant for the subsurface/surface exothermic reactions or a more accurate description of heat release distribution in the fuel/oxidizer diffusion flame above the propellant surface should tend to reduce the sensitivity of predicted burning rate to oxidizer particle size, as desired. Thus far, only the former approach has been examined and has been found to permit selection of a set of constants which gives good agreement between predicted and measured burning rate versus pressure curves for all three particle sizes for the case of no crossflow. In all cases, however, the predicted sensitivity of burning rate to crossflow velocity is somewhat less than observed. It must be stressed that these results are very preliminary and that further examination and optimization of the model is in progress.

Nomenclature

AFU	Fuel surface area	$\dot{m}_{ox,p}$	oxidizer mass flux, based on planar surface projection
APOX	planar projection of exposed oxidizer particle surface area	$\dot{m}_{ox,s}$	oxidizer mass flux, based on actual total curved surface area
ASOX	Total curved oxidizer exposed surface area	MW_{fuel}	molecular weight of fuel gases leaving propellant surface
B_{fuel}	Pre-exponential in fuel pyrolysis mass flux expression	MW_{ox}	Molecular weight of oxidizer gases leaving propellant surface
B_{ox}	Pre-exponential in oxidizer sublimation mass flux expression	n	Global gas-phase reaction order
B_{sub}	Pre-exponential for subsurface reaction rate equation	P	Pressure
C_p	Gas heat capacity (function of oxidizer/fuel ratio)	\dot{q}_{gas}	Total heat flow to surface from gas-phase reactions (energy/time)
$C_{p,fuel}$	Solid fuel heat capacity	$\dot{q}_{diffusion\ flame}$	Heat flux to surface from fuel-oxidizer gas flame (energy/area/time)
$C_{p,ox}$	Solid oxidizer heat capacity	$\dot{q}_{series\ flame}$	Heat flux to surface from combined monopropellant and fuel-oxidizer gas flames (energy/area/time)
C_1	initial net (excess of oxidizer over fuel molecules) molar concentration of oxidizer in the oxidizer decomposition product gases	\dot{q}_{sub}	Heat release via subsurface reactions (energy/time)
C_2	initial molar concentration of fuel in the binder pyrolysis product gases.	Q_{AP}	Heat release associated with $HClO_4(g) + NH_3(g) \rightarrow$ Equilibrium Products
D	Gas diffusivity	Q_{EXO}	heat release per unit mass of oxidizer consumed in surface/subsurface reactions
D_1	Characteristic lattice dimension in regular oxidizer-particle array	$Q_{melt,f}$	heat of melting of binder
D_0	Oxidizer particle diameter	$Q_{melt,ox}$	heat of melting of oxidizer
$D_{channel}$	Flow port hydraulic diameter	$Q_{fuel,vap}$	heat of pyrolysis of fuel binder
DELOX	Distance of center of oxidizer surface from initial oxidizer peak (See Fig. 1)	Q_{subl}	heat of sublimation of oxidizer
EACT,OF	Activation Energy for the fuel-oxidizer gas reaction	R_{α}	fraction of AP reacted per unit time in subsurface reactions
E_{fuel}	Activation Energy for fuel pyrolysis	RBS	outer radius of fuel annular gas column
E_{ox}	Activation Energy for oxidizer sublimation	r_{fuel}	linear regression rate of fuel surface
E_{sub}	Activation Energy for subsurface reaction rate equation	r_{ox}	linear regression rate of oxidizer, normal to its surface
FH90	Distance required for mixing of fuel and oxidizer gas streams	SMRBO	stoichiometric ratio (mass) of binder to oxidizer
i	Stoichiometric moles of fuel per mole of oxidizer	T	temperature
K_{AP}	Constant in expression for oxidizer monopropellant reaction distance	T_f	flame temperature
K_{OF}	Constant in expression for oxidizer-fuel gas reaction distance	T_0	propellant bulk temperature
L_{AP}	Oxidizer monopropellant gas reaction distance	T_s	surface temperature
L_{BS}	Oxidizer gas column radius	TAU	time for fuel regression plane to move from one increment to the next
L_{RX}	Oxidizer-Fuel gas reaction distance	$\bar{U}_{crossflow}$	mainstream crossflow velocity
\dot{m}	Average surface mass flux (based on planar area) at a given increment	$U_{crossflow,x}$	linear gas crossflow rate at distance FH90 sin θ from the surface
\dot{m}_{fuel}	mass flux of fuel	$U_{gas,x}$	linear gas flow rate away from propellant at distance FH90 sin θ from the surface
		U^+	dimensionless crossflow velocity at $x = FH90 \sin \theta$
		$V_{gas,surf}$	gas velocity away from propellant surface
		VLO	volumetric fraction of oxidizer in propellant
		WFO	weight fraction of oxidizer in propellant
		X	distance from surface (sign convention such that it is negative below the surface)
		XDTOP	distance of fuel surface from initial peak of oxidizer particle (See Fig. 1).
		Y^+	dimensionless value of FH90 sin θ
		$Y_{2,0}$	mole fraction of fuel in binder-pyrolysis products in absence of subsurface reactions.
		$Y_{1,0}$	net mole fraction of oxidizer in oxidizer decomposition products in absence of subsurface reactions (corrected for fuel mole fraction initially in the oxidizer stream, e.g., NH_3 , which negates part of the oxidizing value)
		γ	mass fraction of oxidizer which reacts at or below the surface
		β	mass fraction of binder which reacts at or below the surface
		θ	angle between resultant velocity vector and planar surface (See Fig. 2).

λ gas thermal conductivity
 λ_{ox} solid oxidizer thermal conductivity
 ρ_f fuel (binder) density
 ρ_{ox} oxidizer density
 $\rho_{propellant}$ propellant density
 ϕ (actual molar fuel/oxidizer ratio)/(stoichiometric molar fuel/oxidizer ratio)

References

1. King, M.K., "A Model of the Erosive Burning of Composite Propellants," AIAA/SAE 13th Propulsion Conference, Orlando, Florida, July, 1977. AIAA Paper 77-930.
2. Beckstead, M.W., Derr, R.L., and Price, C.F., "The Combustion of Solid Monopropellants and Composite Propellants," 13th International Symposium on Combustion, The Combustion Institute, Pittsburgh, PA, 1971, pp. 1047-1056.
3. Beckstead, M.W., Derr, R.L., Cohen, N.S., et al, "Combustion Tailoring Criteria For Solid Propellants," Lockheed Propulsion Company, Lockheed Report 835F, AFRPL-TR-69-190, May, 1969.
4. Waesche, R.H.W., and Wenograd, J., "Calculation of Solid Propellant Burning Rates From Condensed-phase Decomposition Kinetics," AIAA 7th Aerospace Sciences Meeting, January, 1969, AIAA Paper 69-145. Also, United Aircraft Final Report on Research Investigation of the Decomposition of Composite Solid Propellants, Report H910457-37, Sept., 1969.
5. Burke, S.P., and Schumann, T.E.W., "Diffusion Flames," Ind. and Eng. Chem., 20, 10, p. 998, Oct., 1928.
6. King, M.K., "An Analytical and Experimental Study of the Erosive Burning of Composite Propellants and Modeling of Single Particle Aluminum Combustion," Final Report for AFOSR Contract F44620-76-C-0023, Atlantic Research Corporation, ARC Report No. TR-PL-5673, AFOSR Report No. not yet assigned, Nov., 1976.

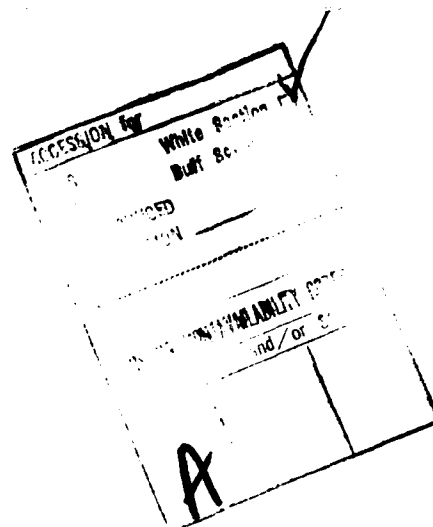


Table 1. Variation of Oxidizer Planer Surface Intersection Area and Associated Fuel Surface Area with Distance of Intersection Plane from Top of the Particle - Typical Case

PARTICLE DIAMETER - 20 MICRONS
 WEIGHT FRACTION OXIDIZER - 0.73
 OXIDIZER DENSITY - 1.96 gm/cm³
 BINDER DENSITY - 0.92 gm/cm³
 VOLUMETRIC OXIDIZER LOADING - 58.05 PERCENT
 D₁ - 21.91 MICRONS

INCREMENT NUMBER	XDTOP DISTANCE FROM TOP OF PARTICLE (MICRONS)	APOX PLANAR OXIDIZER INTERSECTIONAL AREA (MICRONS) ²	AFU PLANAR FUEL AREA (MICRONS) ²
1	0.119	7.4	19.1
2	1.017	90.6	147.2
3	1.915	108.8	280.4
4	2.813	161.9	283.8
5	8.712	189.9	226.8
6	4.610	222.9	192.8
7	5.508	250.8	166.0
8	6.407	273.6	142.1
9	7.305	291.3	124.4
10	8.203	304.0	111.7
11	9.101	311.6	104.1
12	10.0	314.2	101.5
13	10.899	311.6	104.1
14	11.797	304.0	111.7
15	12.695	291.3	124.4
16	13.593	273.6	142.1
17	14.492	250.8	166.0
18	15.390	222.9	192.8
19	16.288	189.9	226.8
20	17.187	161.9	283.8
21	18.085	108.8	280.4
22	18.983	90.6	147.2
23	19.881	7.4	19.1

Table 2. Values of Various Constants Used for an HTPB/AP Formulation.

B _{fuel}	5500 gm/cm ² sec
B _{ox}	200,000 gm/cm ² sec
C _{p, fuel}	0.3 cal/gm °K
C _{p, ox}	0.4 cal/gm °K
D	1.0 (10 ⁻⁵) T ^{1.5} /P cm ² /sec, T in °K, P in atm
E _{ACT, OF}	11000 cal/mole
E _{fuel}	16900 cal/mole
E _{sub}	40000 cal/mole
E _{ox}	22000 cal/mole
i	0.6
MW _{fuel}	19 gm/gm-mole
MW _{ox}	36 gm/gm-mole
Q _{AP}	810 cal/gm (exothermic)
Q _{EXO}	1150 cal/gm (exothermic)
Q _{melt, f}	0
Q _{melt, ox}	30 cal/gm (endothermic)
Q _{fuel, vap}	433 cal/gm (endothermic)
Q _{subl}	450 cal/gm (endothermic)
SMRBO	0.111
λ	5.5 (10 ⁻⁶) [(T _f + T _g) / 2] ^{0.5} cal/cmsec °K
λ _{ox}	0.001 cal/cm sec °K
ρ _f	0.92 gm/cm ³
ρ _{ox}	1.96 gm/cm ³
Y _{2,0}	0.98
Y _{1,0}	0.28

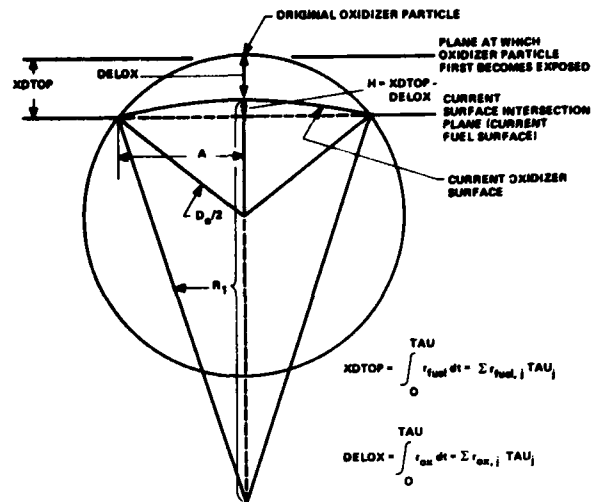


Figure 1. Schematic Demonstrating Calculation of Oxidizer Surface Area at Some Time, TAU, After First Exposure of the Top of the Oxidizer Particle.

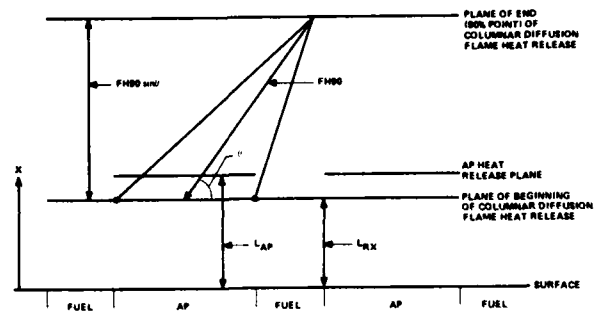


Figure 2. Schematic Showing Key Dimensions Relating to Gas-Phase Heat Release.

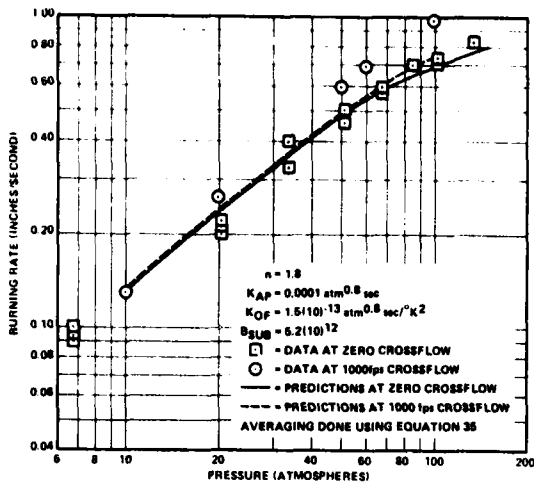


Figure 3. Predicted and Experimental Burning Rates for Formulation 4685 (73/27 AP/HTPB, 5 Micron Diameter AP) Using Initial Estimates for Subsurface Reaction Constants.

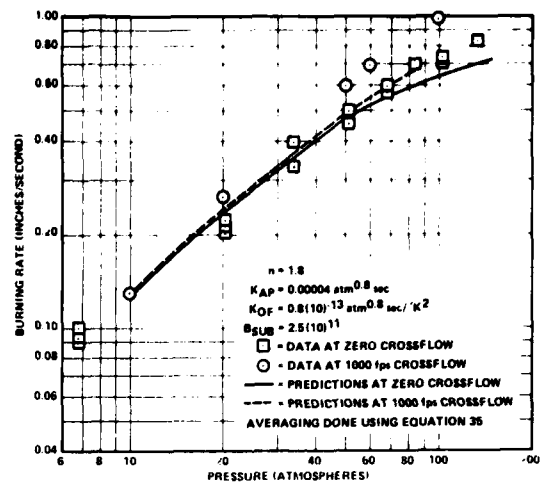


Figure 6. Predicted and Experimental Burning Rates for Formulation 4685 (73/27 AP/HTPB, 5 Micron Diameter AP) Using Optimized Estimate for Subsurface Reaction Pre-exponential.

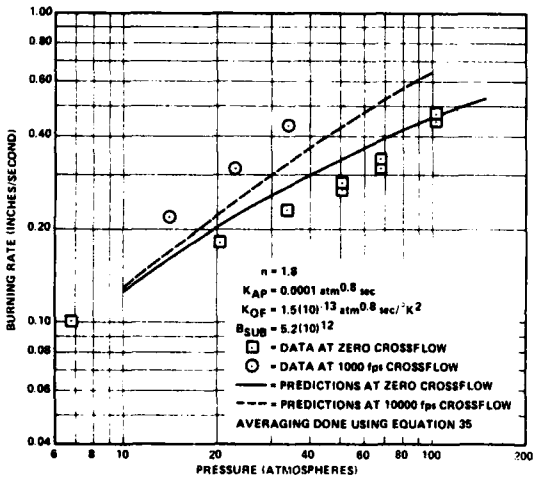


Figure 4. Predicted and Experimental Burning Rates for Formulation 4525 (73/27 AP/HTPB, 20 Micron Diameter AP) Using Initial Estimates for Subsurface Reaction Constants.

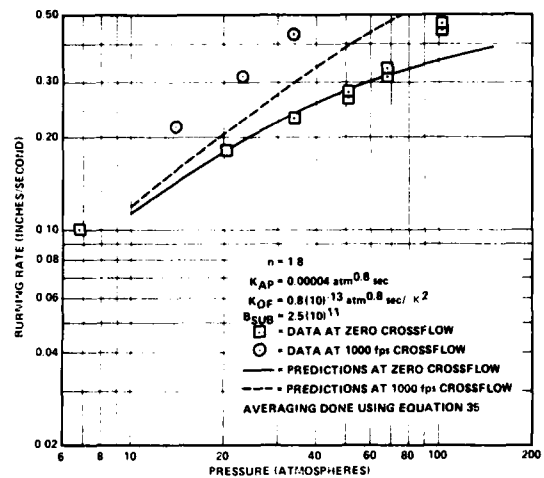


Figure 7. Predicted and Experimental Burning Rates for Formulation 4525 (73/27 AP/HTPB, 20 Micron Diameter AP) Using Optimized Estimate for Subsurface Reaction Pre-exponential.

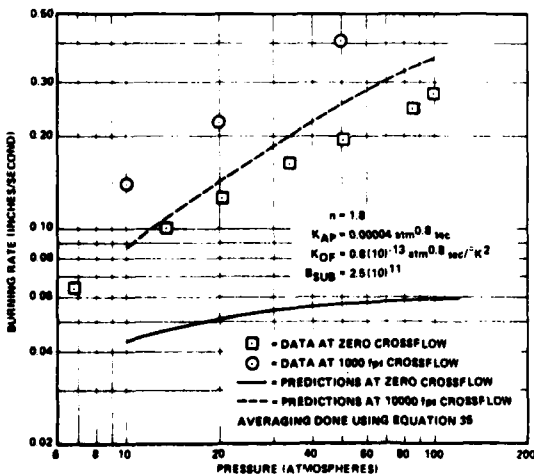


Figure 5. Predicted and Experimental Burning Rates for Formulation 5051 (73/27 AP/HTPB, 200 Micron Diameter AP) Using Initial Estimates for Subsurface Reaction Constants.

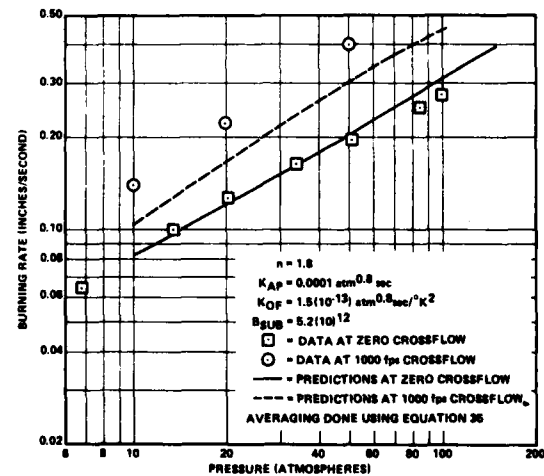


Figure 8. Predicted and Experimental Burning Rates for Formulation 5051 (73/27 AP/HTPB, 200 Micron Diameter AP) Using Optimized Estimate for Subsurface Reaction Pre-exponential.

1 REPORT DOCUMENTATION PAGE		READ INSTRUCTIONS BEFORE COMPLETING FORM	
18 AFOSR/TR-79-0484		2 GOVT ACCESSION NO.	3 RECIPIENT'S CATALOG NUMBER
6	4 TITLE (and Subtitle) Model For Steady-State Combustion of Unimodal Composite Solid Propellants	5 TYPE OF REPORT & PERIOD COVERED Interim rept.	
7 AUTHOR(s) 10 Merrill K./King		8 CONTRACT OR GRANT NUMBER(s) 15 F49620-78-C-0016, F44620-76-C-0023	
9 PERFORMING ORGANIZATION NAME AND ADDRESS Atlantic Research Corporation 5390 Cherokee Avenue Alexandria, VA 22314		PROGRAM ELEMENT PROJECT, TASK AREA & WORK UNIT NUMBERS 16 2388A1 17 A1 61102F	
11 CONTROLLING OFFICE NAME AND ADDRESS Air Force Office of Scientific Research/NA Building 410 Bolling AFB, DC 20332		12 REPORT DATE 11 Jan 1978	
14 MONITORING AGENCY NAME & ADDRESS (if different from Controlling Office) 12 14 p.		13 NUMBER OF PAGES 11	
		15 SECURITY CLASS. (of this report) UNCLASSIFIED	
16 DISTRIBUTION STATEMENT (of this Report) Approved for public release; distribution unlimited			
17 DISTRIBUTION STATEMENT (of the abstract entered in Block 20, if different from Report)			
18 SUPPLEMENTARY NOTES			
19 KEY WORDS (Continue on reverse side if necessary and identify by block number) Erosive burning Composite Propellants Propellant Combustion Modeling 403 338 Jm			
20 ABSTRACT (Continue on reverse side if necessary and identify by block number) A model for prediction of burning rate-pressure-crossflow velocity relationships for non-metalized composite propellants containing unimodal oxidizer, given composition and oxidizer particle size, has been developed. This model embodies many of the concepts used in the Beckstead-Derr-Price model, but contains major modifications, including a postulated columnar diffusion flame-bending mechanism for erosive burning. The major part of this paper is devoted to description and discussion of these modifications and to model development. Preliminary predictions of burning rate at various pressures and crossflow velocities			

have been made for a series of three 73/27 ammonium perchlorate (AP)/hydroxy-terminated polybutadiene (HTPB) formulations, with oxidizer particle diameters of 5, 20, and 200 microns, and compared with data for these formulations. With optimization of three "free constants" appearing in the model, it is found to give excellent agreement with no-crossflow burning rate data over the entire range of pressures and particle sizes studied. In all cases, however, the predicted sensitivity of burning rate to crossflow velocity is somewhat less than observed experimentally.